NUMERICAL INVESTIGATION OF THERMAL HAZARDS FROM UNDER-EXPANDED HYDROGEN JET FIRES USING A NEW SCHEME FOR THE ANGULAR DISCRETIZATION OF THE RADIATIVE INTENSITY

Momferatos, G.[1], Venetsanos, A.G.[2] and Russo, P.[3]
[1] Environmental Research Laboratory, National Center for Scientific Research "Demokritos", Patr. Gregoriou E & 27 Neapoleos Str., Athens, 15341, Greece, g.momferatos@ipta.demokritos.gr
[2] Environmental Research Laboratory, National Center for Scientific Research "Demokritos", Patr. Gregoriou E & 27 Neapoleos Str., Athens, 15341, Greece, venets@ipta.demokritos.gr
[3] Department of Chemical Engineering Materials Environment, University of Rome "La Sapienza", 18 Eudosianna Str., Rome, 00184, Italy, paola.russo@uniroma1.it

ABSTRACT

In the context of a numerical investigation of thermal hazards from two under-expanded hydrogen jet fires, results from a newly-developed thermal radiation module of the ADREA-HF computational fluid dynamics (CFD) code were validated against two physical experiments. The first experiment was a vertical under-expanded hydrogen jet fire at 170 bar, with the objective of the numerical investigation being to capture the spatial distribution of the radial radiative heat flux at a given time instant. In the second case, a horizontal under-expanded hydrogen jet fire at 340 bar was considered. Here, the objective was to capture the temporal evolution of the radial radiative heat flux at selected fixed points in space. The numerical study employs the eddy dissipation model for combustion and the finite volume method (FVM) for the calculation of the radiative intensity. The FVM was implemented using a novel angular discretization scheme. By dividing the unit sphere into an arbitrary number of exactly equal angular control volumes, this new scheme allows for more flexibility and efficiency. A demonstration of numerical convergence as a function the number of both spatial and angular control volumes was performed.

1.0 NOMENCLATURE

$\hat{n}$	Unit spatial vector
$I(\vec{r},\hat{s})$	Radiative intensity
$\vec{r}$	Coordinate vector
$\hat{s}$	Unit angular vector
$\kappa(\vec{r})$	Absorption coefficient
$I_b(\vec{r})$	Blackbody emission
σ	Stefan-Boltzmann constant
T	Temperature
$\beta(\vec{r})$	Extinction coefficient
$\sigma_s(\vec{r})$	Scattering coefficient
$\Phi(\vec{r},\hat{s},\hat{s}')$	Scattering phase function
N	Total number of angular control volumes
N_φ	Number of polar belts
N_θ	Number of azimuthal zones

L_{vis}	Visible flame length
t	time
X_{H_2}	Hydrogen volume concentration

2.0 INTRODUCTION

High-pressure hydrogen compression is the main currently chosen technology for onboard storage in vehicle tanks. An accidental hydrogen release from a damaged storage system or from a thermal pressure relief device (TPRD) may ignite, resulting in a jet fire with a flame length of the order of tens of meters. The resulting high temperatures of the flame combined with the radiative heat flux propagating away from it clearly present a serious threat for both life and property. This situation calls for the development of predictive engineering tools which will allow one to estimate safety distances and allow the design of safer hydrogen storage systems. One such promising tool is computational fluid dynamics (CFD), which has been proven capable of simulating realistic accident scenarios in hydrogen safety engineering. In the case of hydrogen jet fire scenarios, initial studies focused on the calculation of simple flame characteristics, such as length and width [1–3], with studies including effects of the radiative heat flux from the jet fire appearing more recently [4–6].

This study validates the newly-developed radiation module of the ADREA-HF CFD code against two independent physical experiments. A novel feature of this work is the introduction of a new angular discretization scheme for the radiative intensity. The present paper is organized as follows: first we present our numerical method implemented in the radiation module of ADREA-HF. This is followed by a comparison of experimental and numerical results which validates our method, accompanied by brief descriptions of the physical experiments. This section includes a careful study of the effects of both spatial and angular discretization. The paper closes with a brief section where conclusions are stated.

3.0 NUMERICAL MODEL

The ADREA-HF code [7] was used in all simulations included in this study. It is an in-house finite volume CFD code capable of solving the flow equations in arbitrary geometrical configurations using Cartesian grids and the method of porosities. Due to the simplicity of the geometries considered, the method of porosities was not utilized in this study, because of perfect boundary-grid alignment. The standard k-ε turbulence model was employed in an unsteady Reynolds-averaged Navier-Stokes (URANS) approach, whereas hydrogen non-premixed turbulent combustion was modeled using the eddy-dissipation concept (EDC) model [8]. The timestep of all simulations was controlled with the use of a Courant-Friedrichs-Lewy (CFL) condition, with a CFL number equal to 2.0. The finite volume method (FVM) [9] was chosen for the calculation of radiative heat transfer. This choice was done after a careful comparison of the FVM with the P1 radiation model [9], which was found to perform poorly. This comparison is not presented here.

The FVM discretizes the radiative transfer equation (RTE):

$$\hat{n}\cdot\vec{\nabla}I(\vec{r},\hat{s}) = \kappa(\vec{r})I_b(\vec{r}) - \beta(\vec{r})I(\vec{r},\hat{s}) + \frac{\sigma_s(\vec{r})}{4\pi}\int_{4\pi} I(\vec{r},\hat{s})\Phi(\vec{r},\hat{s},\hat{s}')d\Omega', \quad (1)$$

where $I(\vec{r},\hat{s})$ is the radiative intensity (W/m^2/sr), $\kappa(\vec{r})$ is the absorption coefficient (m^{-1}), $I_b(\vec{r}) = \sigma\frac{T^4(\vec{r})}{\pi}$ is the blackbody emission (W/m^2/sr) which depends on the temperature distribution $T(r)$ (K), $\beta(\vec{r}) = \kappa(\vec{r}) + \sigma_s(\vec{r})$ is the extinction coefficient (m^{-1}), $\sigma_s(\vec{r})$ is the scattering coefficient (m^{-1}) and finally $\Phi(\vec{r},\hat{s},\hat{s}')$ is the non-dimensional scattering phase function. In hydrogen combustion, complete absence of soot implies a zero scattering coefficient, so the last term in (1) is neglected. The RTE evidently depends on the temperature distribution, which is provided by the URANS equations. The

absorption coefficient $\kappa(\vec{r})$ and the extinction coefficient $\beta(\vec{r})$ are calculated as functions of temperature using the improved model first presented in [10].

The angular dependency of the radiative intensity $I(\vec{r},\hat{s})$ is discretized by subdividing the unit sphere into N angular control volumes (ACVs). The particular choice of this discretization is a non-trivial matter [9]. The "naive" approach which involves subdividing the unit sphere into N_φ polar belts times N_θ azimuthal zones (Figure 1, left) can result in large surface ratios between ACVs located near the equator and ACVs located near the poles, a fact which can lead to loss of numerical precision. The FT_N scheme first presented in [11] partly remedied this deficiency by considering a variable number of ACVs per polar belt. An example of this discretization scheme is presented in (Figure 1, centre). In this scheme, for N_φ different polar angles one subdivides each polar belt into equal sectors according to the distribution $4, 8, .., 2N_\varphi - 4, 2N_\varphi, 2N_\varphi - 4, ..., 8, 4$. However, the FT_N scheme does not allow the use of an arbitrary number of ACVs. In particular, the total number of ACVs must be equal to $N = N_\varphi(N_\varphi + 2)$, where N_φ must be even. Clearly this can be a practical disadvantage in some situations, particularly in problems where the angular resolution must be increased under constraints in computer memory or available computational time. On the numerical side, the FT_N scheme only enforces approximate equality on the ACVs, a fact which can also be a drawback in some demanding problems involving large temperature gradients.

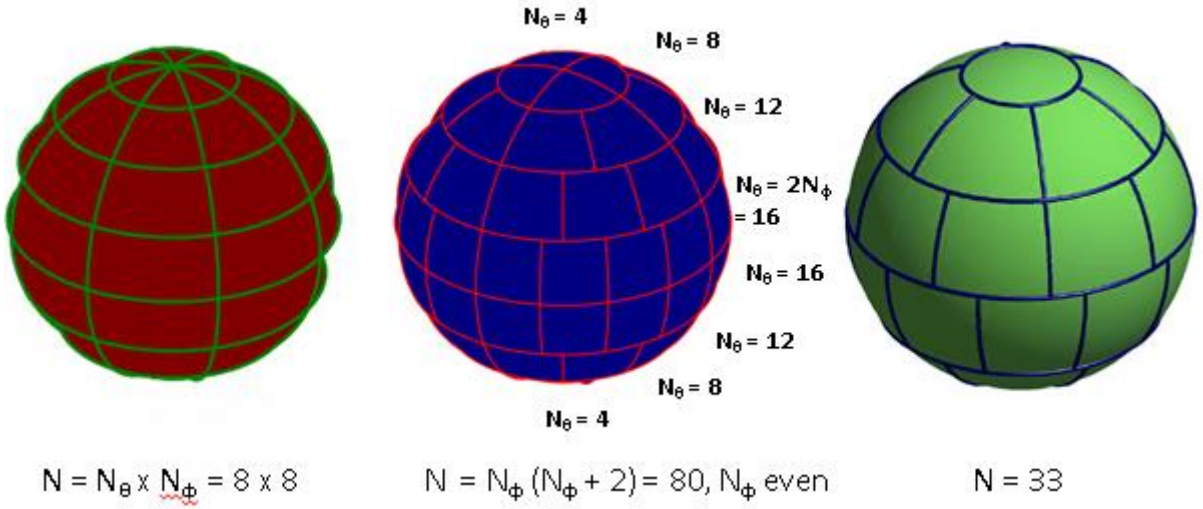

Figure 1. Three different angular discretization schemes. Left: Unequal subdivision. Middle: Almost equal subdivision (FT_N scheme). Left: Our proposed scheme (exactly equal subdivision).

In this study, we propose a new angular discretization scheme which is based on the geometrical algorithm first published in [12]. This algorithm subdivides the unit sphere into an arbitrary number of sectors of exactly equal surface area (Figure 1, right), which we utilize as ACVs in our FVM. The advantage of the method we propose is twofold: on the practical side, the total number of ACVs is arbitrary (instead of being constrained in the case FT_N). As far as numerical precision is concerned, the exact equality of ACVs is a potential advantage in demanding problems with large temperature gradients.

For all simulations presented in this work, completely quiescent atmospheric air with zero turbulence levels was used as an initial condition. Non-reflective boundary conditions were applied in all free planes not intersecting the jet axis, while n the upstream and downstream free planes zero gradient boundary conditions were applied. In the lower ground plane, appropriate Cauchy boundary conditions with standard wall functions for turbulence were used. Radiation boundary condition were as follows: zero gradient boundary conditions were applied in all free planes, and standard blackbody emission

boundary condition was used in the ground plane. Combustion was initiated at the vicinity of the nozzle by instantaneously igniting a small volume of gas inside which the X_{H_2} was above 4%.

4.0 RESULTS AND DISCUSSION

4.1 Vertical Under-Expanded Jet Fire

The first experiment considered is a vertical under-expanded jet fire at 170 bar [13,14]. A sketch of the experimental setup is shown in Figure 2. The diameter of the nozzle is equal to 1.91 mm. Blowdown was initiated from a set of 6 hydrogen tanks at a pressure of approximately 2500 psia. During the experiment, the flame length L_{vis} was measured at various time instants and a set of radiometers was accordingly placed at an axial distance equal to $L_{vis}/2$. This makes the radial radiative heat flux at this fixed non-dimensional radial distance available as a function of height, at various time instants. In this study, we select the first recorded time instant at 5 s after ignition for validation against our numerical results.

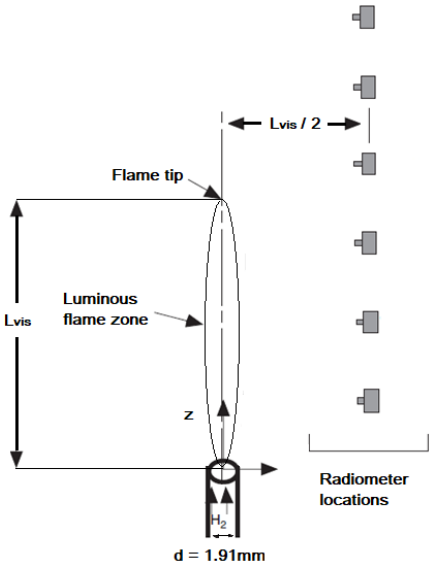

Figure 2. Sketch of the vertical under-expended jet flame experiment (adapted from [13]).

In all simulations presented in this section, the simulation domain was extended 3.5 m away from the nozzle in x and y directions, and 12 m in the z direction. The grid remained uniform up to 0.13 m in the x and y directions and 0.26 m in the z direction, consisting of cubical spatial control volumes (SCVs) of side equal to 0.026, 0.0173 and 0.0144 m for the coarse, medium and dense grid respectively. Outside the aforementioned limits, the sides of the SCVs expanded with a ratio equal to 1.12 for all three space directions.

In comparing our numerical results with the vertical under-expanded jet fire experiment of [13,14], our main objective is to answer the following question: how well can our radiation model predict the spatial distribution of the radiative heat flux at a fixed time instant? In Figure 3 we present a comparison of the predictions of the radial radiative heat flux q_x at a radial distance equal to $L_{vis}/2$ and t = 5 s, as a function on non-dimensional height, for two different angular discretization schemes: the FT_N scheme and our new proposed scheme. The number of ACVs is equal to N = 80 and the spatial grid is composed of approximately 162,000 SCVs. The experimental visible flame length L_{vis} at t = 5.0 s is equal to 4.3 m, whereas our simulations predict a value between 4.7 and 4.9 m which does not vary with angular discretization scheme, angular or spatial resolution. The lower value corresponds to the distance of the furthest T = 1500 K temperature contour from the nozzle, whereas

the upper limit corresponds to the distance to the furthest T = 1300 K temperature contour. For all curves, the non-dimensional height is normalized by dividing with the experimental visible flame length. We observe that both angular discretization schemes capture the curve of the radial radiative heat flux rather accurately, especially for small values of non-dimensional height, and that the new scheme performs marginally better overall. The discrepancy at the right tail of the curve can be attributed to the influence of boundary conditions, as well as, to some extent, the difference between the experimental and numerical flame length.

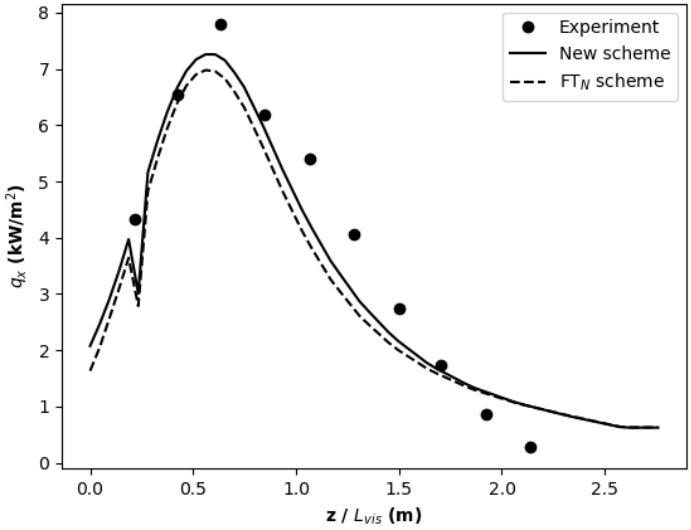

Figure 3. Vertical jet fire experiment: numerical predictions for the radial radiative heat flux as a function of non-dimensional height. Circles: experimental measurements. Dashed line: FT_N scheme. Solid line: our new proposed scheme.

In Figure 4, we consider the independence of our new angular discretization scheme with respect to the number of ACVs. For this purpose, we present again the predictions for the radial radiative heat flux as above but for three different angular discretizations: a coarse one with 80 ACVs, a medium one with 120 ACVs and a fine one with 168 ACVs. The spatial grid is the same as in Figure 3, consisting of 162,000 SCVs. It is evident that the new scheme demonstrates excellent convergence properties, as the three curves corresponding to the coarse, medium and fine angular discretizations are very close to each other.

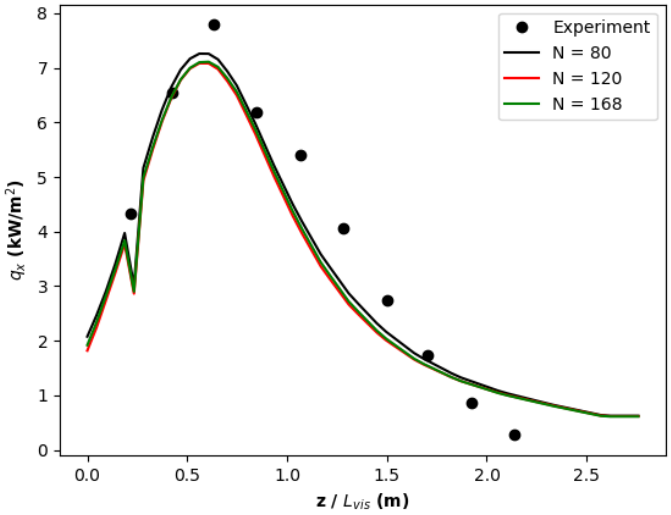

Figure 4. Vertical jet fire experiment: demonstration of independence of numerical results with respect to the number of ACVs. Circles: experimental measurements. Black: N = 80 ACVs. Red: N = 120 ACVs. Green: N = 168 ACVs.

Figure 5 presents a spatial grid independence study for our new angular discretization scheme. In all curves the number of ACVs is equal to N = 80. The coarse grid is the same as in the previous two figures (162,000 SCVs), the medium grid is composed of approximately 272,000 SCVs and the fine grid is composed of approximately 358,000 SCVs. As the spatial resolution changes from coarse to medium, the peak of the curve is more accurately captured, whereas the predictions for small values of non-dimensional height remain excellent. As the spatial resolution changes from medium to dense, the peak of the curve is slightly under-predicted. Comparing the coarse grid with the two denser ones, predictions are significantly improved for intermediate values of non-dimensional height (1-1.5), while for higher values the discrepancy remains. This suggests that the source of this disagreement between experiment and simulation is due to boundary conditions and numerical/experimental visible flame length differences.

The dip occurring at $zL_{vis}^{-1} \cong 0.25$, which is present in almost all cases shown in Figure 3-5 (with the medium grid in Figure 5 being an exception), is presumably due to ray effects [15]. In the FVM, ray effects can result in an under-prediction of the radiative intensity (and thus also of the radiative heat flux) when radiation from an area which is limited in space, such as a jet, is propagated in the discrete set of directions defined by the ACVs [16]. The absence of the dip for the medium grid in Figure 5 is compatible with the hypothesis that the under-prediction is due to ray effects, as they in general depend on the details of the spatial and angular discretizations.

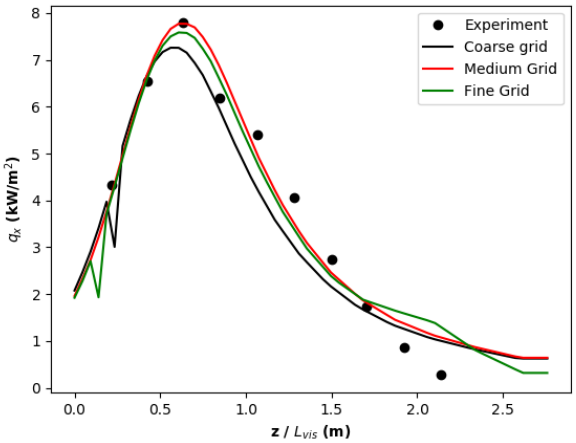

Figure 5. Vertical jet fire experiment: demonstration of independence of numerical results with respect to number of SCVs. Circles: experimental measurements. Black line: coarse grid. Red line: medium grid. Green line: fine grid.

4.2 Horizontal Under-Expanded Jet Fire

In the second experiment, a horizontal under-expanded jet fire at 340 bar was studied. This experiment was performed by the University of Rome "La Sapienza" in collaboration with the Italian Fire Corps within the framework of the HyTunnel-CS project. In Figure 6, we present a sketch of the experimental setup. The diameter of the nozzle is equal to 1 mm. Neither blowdown curves nor flame lengths were measured during the experiment. Three radiometers were positioned at the horizontal plane passing through the nozzle (z = 1.05 m). This configuration makes the value of the radiative heat flux available as function of time at three different fixed locations. As seen in Figure 6, this experiment included several thermocouples, however temperature measurements are not considered in this study, which focuses on the radiative heat flux.

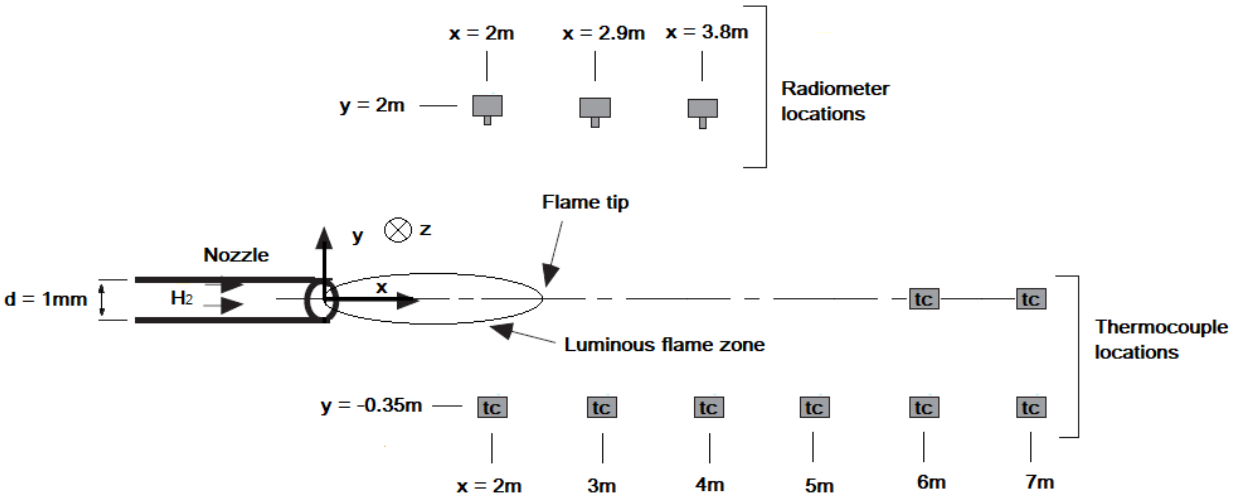

Figure 6. Sketch of the horizontal under-expended jet flame experiment

For the simulations presented in this subsection the computational domain extended 3 m away from the jet axis in the positive and negative y direction. In the x direction, it extended 3 m upstream and 10 m downstream, while in the z direction it extended 4 m above the jet. The grid remained uniform in a region of dimensions (x, y, z) = (0.4, 0.012, 0.012) m located in front of the nozzle. There, all SCVs

were cubical with a side equal to 0.04, 0.02 and 0.0133 m for the coarse, medium and dense grid respectively. Outside this region the sides of the SCVs were expanded with a ratio equal to 1.12 in all spatial directions.

The horizontal under-expanded jet fire experiment provides an opportunity to test our radiation model's predictions of the radiative heat flux as a function of time, at three different fixed points in space. In Figure 7 we present the predictions of the radial radiative heat flux as a function of time given by the two different angular discretization schemes. The number of ACVs is equal to N = 168, whereas the number of SCVs is approximately equal to 129,000. Both schemes are able to capture the values given by all three radiometers during the whole duration of the experiment.

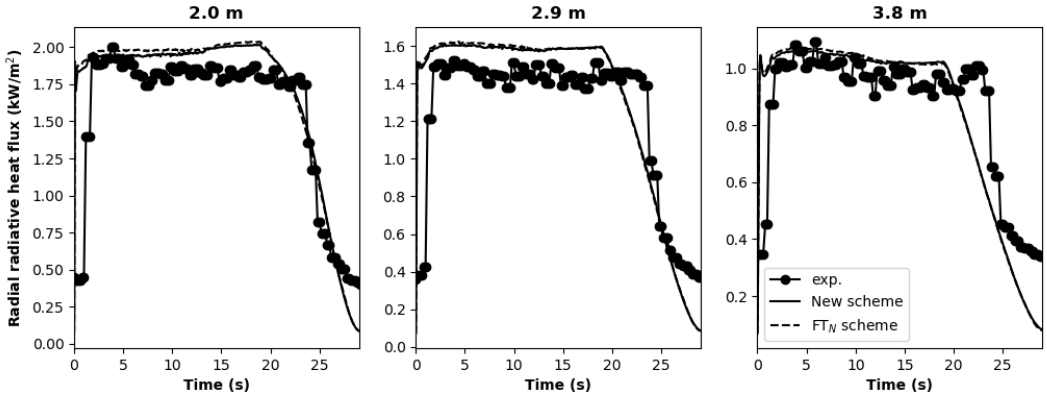

Figure 7. Horizontal jet fire experiment: comparison of the predictions of the radial radiative heat flux as a function of time given by the two different angular discretization schemes. Filled circles: experimental measurements. Dashed line: FT_N scheme. Solid line: Our new proposed scheme. Left: First radiometer, x = 2 m from the nozzle. Middle: x = 2.9 m from the nozzle. Right: x = 3.8 m from the nozzle.

Figure 8 demonstrates the independence of the numerical predictions for the radial radiative heat flux with respect to the angular discretization, for the horizontal jet flame experiment. Results corresponding to three different angular discretizations are presented: the coarse one corresponds to N = 168 ACVs, the medium to N = 224 ACVs and the fine one to N = 288 ACVs. The number of SCVs is again approximately equal to 129,000. Even though the predictions corresponding to the coarse and medium angular discretizations are closer to the experimental curves than the prediction corresponding to the fine angular discretization, all numerical curves remain close to the experimental ones for all radiometer positions. This is, overall, a more demanding problem than the vertical jet fire, as is evidenced by the increased number of ACVs which is necessary to reproduce the experimental curves.

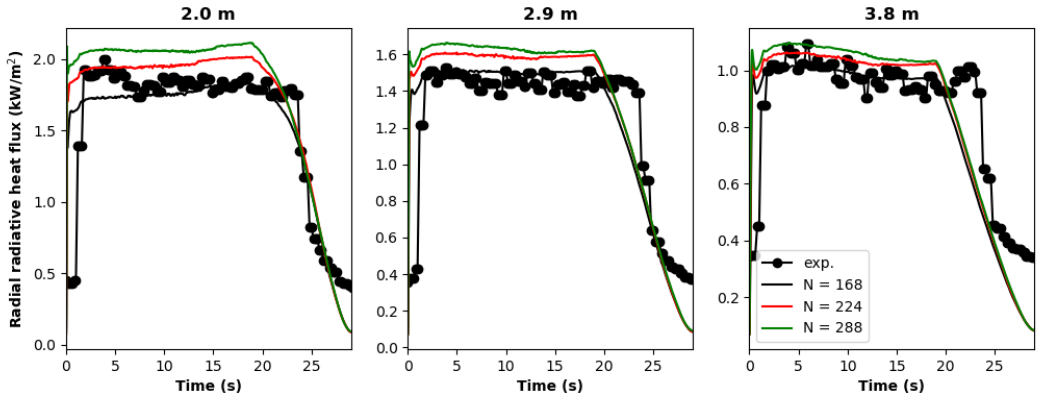

Figure 8. Horizontal jet fire experiment: demonstration of independence of numerical results with respect to the number of ACVs. Circles: experimental measurements. Black: N = 168 ACVs. Red: N = 224 ACVs. Green: 288 ACVs. Left: First radiometer, 2 m from the nozzle. Middle: 2.9 m from the nozzle. Right: 3.8 m from the nozzle.

Finally, in Figure 9 we present a spatial grid independence study for the horizontal jet flame experiment. Again, we consider the radial radiative heat flux as a function of time at the same three different positions. The coarse grid is the same as in the previous two figures, consisting of approximately 129,000 SCVs, the medium grid consists of approximately 365,000 SCVs spatial control volume and the fine grid of approximately 650,000 SCVs, whereas the number of ACVs is equal to 224 in all cases. Numerical convergence is satisfactory overall, since all curves remain close to the experimental measurements for the whole duration of the experiment and the numerical predictions of the two finer grids are improved, especially for the radiometers located at x = 2.9 m and y = 3.8 m (middle and right sub-figures in Figure 9). As the spatial resolution is increased, the spurious trend observed in Figure 8 (i.e. the coarse and medium angular discretizations being closer to the experimental curves than the fine one) is remedied.

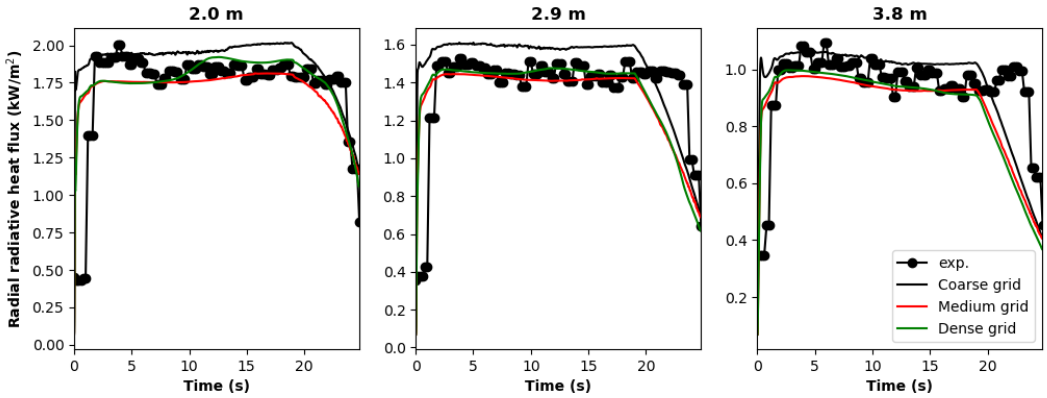

Figure 9. Horizontal jet fire experiment: demonstration of independence of numerical results with respect to the number of SCVs. Filled circles: experimental measurements. Black: coarse grid. Red: medium grid. Green: fine grid. Left: First radiometer, x = 2 m from the nozzle. Middle: x = 2.9 m from the nozzle. Right: x = 3.8 m from the nozzle.

In an extrapolation from the available experimental data, we also explored a larger diameter horizontal jet fire case with a setup in all other respects identical with the jet fires presented in this subsection. As a simple validation test, we compared the numerically predicted visible flame length with the one predicted by the NET e-laboratory online tool [17], which utilizes the correlation model presented in [18]. The numerically predicted visible flame is in the range [4.92, 6.05] m while the engineering model predicts a larger visible flame length equal to 6.23 m. The numerically predicted radiative heat

fluxes at the three sensor positions (x = 2.0, 2.9 and 3.8 m) stabilize early at the quite elevated values of 13.73, 17.31 and 18.24 kW/m^2. Numerical convergence of the radiative heat flux curves versus time with respect to the same numbers of ACVs as above (not shown) was found to be excellent.

5.0 CONCLUSIONS

The newly developed radiation module of the ADREA-HF code was validated against results from two independent physical experiments. In both cases, we have demonstrated that our new angular discretization scheme performs as good as the state-of-the-art scheme of [11]. For both experiments, a careful independence study of the numerical results with respect to both angular and spatial resolution was performed, with excellent results. The new discretization scheme has a twofold advantage over the pre-existing ones, an advantage which is not particular to the ADREA-HF code but one that could benefit any CFD code with radiative heat transfer, including codes utilizing unstructured meshes. Firstly, it is more practical, since it allows for the subdivision of the unit sphere in an arbitrary number of ACVs. Secondly, these ACVs are of exactly equal surface area, a fact that is expected to be a numerical advantage in more demanding problems with large temperature gradients. However, this second advantage remains to be demonstrated in a future study involving such more demanding problems.

6.0 AKNOWLEDGEMENTS

The research leading to these results was financially supported by the HyTunnel-CS which has received funding from the Fuel Cells and Hydrogen 2 Joint Undertaking under grant agreement No 826193. This Joint Undertaking receives support from the European Union's Horizon 2020 research and innovation program, Hydrogen Europe and Hydrogen Europe research. This work was supported by computational time granted from the National Infrastructures for Research and Technology S.A. (GRNET S.A.) in the National HPC facility - ARIS - under project ID pr0008027-HSETUP.

7.0 REFERENCES

[1] Brennan SL, Makarov D V., Molkov V. LES of high pressure hydrogen jet fire. J Loss Prev Process Ind 2009;22:353–9. https://doi.org/10.1016/j.jlp.2008.12.007.

[2] Houf WG, Evans GH, Schefer RW. Analysis of jet flames and unignited jets from unintended releases of hydrogen. Int J Hydrogen Energy 2009;34:5961–9. https://doi.org/10.1016/j.ijhydene.2009.01.054.

[3] Zheng J, Bie H, Xu P, Liu P, Zhao Y, Chen H, et al. Numerical simulation of high-pressure hydrogen jet flames during bonfire test. Int J Hydrogen Energy 2012;37:783–90. https://doi.org/10.1016/j.ijhydene.2011.04.061.

[4] Wang CJ, Wen JX, Chen ZB, Dembele S. Predicting radiative characteristics of hydrogen and hydrogen/methane jet fires using FireFOAM. Int. J. Hydrogen Energy, vol. 39, Elsevier Ltd; 2014, p. 20560–9. https://doi.org/10.1016/j.ijhydene.2014.04.062.

[5] Cirrone DMC, Makarov D, Molkov V. Thermal radiation from cryogenic hydrogen jet fires. Int J Hydrogen Energy 2019;44:8874–85. https://doi.org/10.1016/j.ijhydene.2018.08.107.

[6] Cirrone DMC, Makarov D, Molkov V. Simulation of thermal hazards from hydrogen under-expanded jet fire. Int J Hydrogen Energy 2019;44:8886–92. https://doi.org/10.1016/j.ijhydene.2018.08.106.

[7] Venetsanos AG, Papanikolaou E, Bartzis JG. The ADREA-HF CFD code for consequence assessment of hydrogen applications. Int J Hydrogen Energy 2010;35:3908–18. https://doi.org/10.1016/j.ijhydene.2010.01.002.

[8] MAGNUSSEN B. On the structure of turbulence and a generalized eddy dissipation concept for chemical reaction in turbulent flow, American Institute of Aeronautics and Astronautics (AIAA); 1981. https://doi.org/10.2514/6.1981-42.

[9] Modest MF. Radiative heat transfer. Academic press; 2013.

[10] Chmielewski M, Gieras M. Planck Mean Absorption Coefficients of H2O, CO2, CO and NO for radiation numerical modeling in combusting flows. J Power Technol 2015;95:97–104.

[11] Kim SH, Huh KY. A new angular discretization scheme of the finite volume method for 3-D radiative heat transfer in absorbing, emitting and anisotropically scattering media. Int J Heat Mass Transf 2000;43:1233–42. https://doi.org/10.1016/S0017-9310(99)00211-2.

[12] Leopardi P. A partition of the unit sphere into regions of equal area and small diameter. Electron Trans Numer Anal 2006;25:309–27.

[13] Schefer RW, Houf WG, Bourne B, Colton J. Spatial and radiative properties of an open-flame hydrogen plume. Int J Hydrogen Energy 2006;31:1332–40. https://doi.org/10.1016/j.ijhydene.2005.11.020.

[14] Schefer RW, Houf WG, Williams TC, Bourne B, Colton J. Characterization of high-pressure, underexpanded hydrogen-jet flames. Int J Hydrogen Energy 2007;32:2081–93. https://doi.org/10.1016/j.ijhydene.2006.08.037.

[15] Coelho PJ. The role of ray effects and false scattering on the accuracy of the standard and modified discrete ordinates methods. J Quant Spectrosc Radiat Transf 2002;73:231–8. https://doi.org/10.1016/S0022-4073(01)00202-3.

[16] Li H-S, Flamant G, Lu J-D. MITIGATION OF RAY EFFECTS IN THE DISCRETE ORDINATES METHOD. Numer Heat Transf Part B Fundam 2003;43:445–66. https://doi.org/10.1080/713836241.

[17] NET e-laboratory tool. https://elab-dev.iket.kit.edu/ (accessed June 29, 2021).

[18] Physics and modelling of underexpanded jets and hydrogen dispersion in atmosphere — Ulster University n.d. https://pure.ulster.ac.uk/en/publications/physics-and-modelling-of-underexpanded-jets-and-hydrogen-dispersi-3 (accessed June 29, 2021).